XIV. DESCRIPTION, CLASSIFICATION, AND DISTRIBUTION OF MANGANESE NODULES

Tomoyuki Moritani, Shiuji Maruyama,
Masato Nohara, Katsutoki Matsumoto,
Tsuyoshi Ogitsu, and Hisamitsu Moriwaki

Method of nodule study

Bottom sampling was done at stations spaced over a distance of usually 1° or about 100 km apart and in some detailed survey areas they were more closely spaced. Two types of sampler were used; the larger size grab sampler, "Ocean-70", which can take a bottom portion of about 0.50 m^2 square area and 35 cm deep including both nodules and sediments; and the freefall grab sampler with about 0.13 m^2 catch area and only nodules in its hauls. The sampler is dropped usually in two sets at each site of the Ocean-70 grab sampling. Also, in some places, additional piston coring and sea bottom photographing by deep sea camera were made.

Nodule samples obtained were described and studied on board for 1) observation of occurrence and morphology in and outside samplers, size classification, measurement of weight and calculation of population density (kg/m^2); 2) photographing whole nodules on the plate marked with the frames of unit areas of both Ocean-70 (0.50 m^2) and freefall grab (0.13 m^2), and that of typical samples on the plate with a 5 cm grid scale; 3) observation of internal structures of the nodules on cut section; and 4) determination of mineral composition by X-ray diffractometer. Chemical analysis was carried out in the laboratory after the cruise as described in Chapter XVI of this Report.

The results are summarized in both the sample lists (Table XIV-1) and the photograph log (Fig. XIV-5). Classification of nodules was made by synthesis and comparison of individual observation data at each station. The relation between nodule types and geological environment or chemical composition was examined by referring to other data of related studies, such as sedimentology, acoustic survey, and chemical analysis.

Types of manganese nodules

The manganese nodules sampled in the GH76–1 cruise area are tentatively classified into nine types on the basis of nodule size, shape, and surface texture as shown in Table XIV-2 and Figs. XIV-1 and 2. In the table, a comparison was made with the two existing classification schemes by MEYER (1973) and MEYLAN (1974), which are based on the observation of a more extensive range and number of samples from the Pacific Ocean. Generally, the nodules occur as group of the same or similar types at one station or in one grab haul.

Surface textures

Surface textures are the most important criteria of classification. Generally, nodule occurrence is confined to the sediment-water interface of the sea bottom, in which nodules are buried in the sediments in different degree (Fig. XIV-3). The relative position of occurrence seems to result in a difference in surface texture, namely rough

Table XIV-1 List of sampled and observed manganese nodules of the GH76–1 cruise.

Station no.	Sample no.	Associated sediment type [data by Ocean-70G]	Morphological type	Total weight (kg)	Population density	(kg/m²)	Number of size fraction (mm) >16	16 −8	8 −6	6 −4	4 −2	2 −1	<1	Bulk wet density (g/cm³)	Inner structure, nucleous
403	FG1–2	[Siliceous clay]	V		+	<0.1					1				Pumice coated oxides
405	G169	Siliceous clay	Sr	0.190	⊕	0.4				2	3	7	24	1.5	Pumice
406	FG4–2	[Deep sea clay]	Sr		+	<0.1					1	1			Pumice
406A	G194	Deep sea clay	Sr	0.005	+	<0.1						4	1		
407	G171	Deep sea clay	ISs, V(n.fr.)	15.100	●	30.0		9	40	83	60	3		1.90–2.03	Fractured nodules and phosphatized sediments
	FG5–1		ISs, V(n.fr.)	3.830	●	29.2		2	11	21	15			1.87–1.98	〃
	FG5–2		ISs, V(n.fr.)	3.75	●	29.2		4	8	14	18			1.88–1.94	〃
407A	D137(N)		ISs, V(n.fr.), IDPs	17.80											〃
	C8(N)		[ISs, IDPs]		[●]										
407A–2	FG32–1		Crust, DPs Ss/SPs	0.101	⊕	0.8				(1)	1 (3)	2 (5)	(8)	1.9	Altered volcanic rocks
	FG32–2		SEr, Sr	2.280	◉	17.5			11	3				2.0–2.1	Phosphatized sediments
	FG32–3		Sr	0.150	△	1.2				1	3	5	3	1.8–2.0	〃
	FG32–4		Sr	0.035	⊕	0.3					2	1	1	1.9	〃
	FG32–5		Sr	0.065	⊕	0.5					5	9		1.7–1.9	〃
	FG32–6		Sr	0.043	⊕	0.3					3	4	4	2.0	〃
	FG32–7		Sr	0.169	△	1.3				3	2	10	6	1.7–1.9	〃
	FG32–8		Sr	0.166	△	1.3				2	3	8	1	1.7–1.9	〃
408	G172	Deep sea clay	IDPs, DPs	5.887	◉	11.8		8	8	77	97	12		1.95–2.08	Phosphatized sediments, composit pisolitic nodules
	FG6–1		IDPs, DPs	3.000	●	23.0		2	5	41	36	4			〃
	FG6–2		IDPs, DPs	2.605	●	20.0		2	2	37	51	5			〃
408A	P73	Deep sea clay	DPs	0.017						1				2.1	
408A–1	C7		[IDPs, DPs]		[●]	68–71%									
409	G173	Siliceous clay	Sr	0.225	⊕	0.5				1	7	6	8	1.85–1.97	Small clay particles, shark's teeth
	FG7–1		Sr	0.040	⊕	0.3					2	5	2	1.92	〃
	FG7–2		Sr	0.290	△	2.3				1	10	5	2	2.00–2.19	〃
410	G174	Siliceous clay	Sr	0.009	+	<0.1						3	2	2.0	
	FG8–1		Sr	0.009	⊕	0.1					1	1	1	2.0	
	FG8–2		Sr	0.012	⊕	0.1						3	1	2.18	

Table XIV-1 (continued)

Station no.	Sample no.	Associated sediment type [data by Ocean-70G]	Morphological type	Total weight (kg)	Population density	(kg/m²)	Number of size fraction (mm) >16	16 −8	8 −6	6 −4	4 −2	2 −1	<1	Bulk wet density (g/cm³)	Inner structure, nucleous
411	G175	Deep sea clay	Db, Sr	0.669	△	1.3		2	4	15	23	52		1.87–1.92	Clay
	FG9–1		Sr	0.026	⊕	0.2				2	8	8		1.73	〃
	FG9–2		Sr	0.087	⊕	0.8			1	1	21	35		1.74	〃
412	G176	Siliceous clay	Sr	0.032	⊕	0.1				2	5	2		1.68	Pumice
	FG10–2		Sr	0.016	⊕	0.1				2	2			1.45	〃
414	FG12–1		DPs, IDPs	2.129	◉	16.4		2	19	59	11	3		1.97–2.18	Phosphatized sediments
	FG12–2		DPs, IDPs	2.231	◉	17.2		3	19	52	30	5		2.0	〃
414A	G193	Siliceous clay	DPs	5.355	◉	10.7			54	509	56			1.93–2.02	〃
414A–1	P67														
414A–2	FG25–1		Sr	0.457	△	3.5				24	13	51		1.8–2.1	Manganese oxide particle, small fossils
	FG25–2		Sr	0.280	△	2.2				16	27	3		1.90–2.0	〃
414A–3	C6					25–37%									
417	G181	Deep sea clay	Sr	0.144	⊕	0.3			1	6	3	91		1.8	Clay
	FG15–1		Sr, V(f.)	0.103	⊕	0.8		1	1	3	8	3		2.1	Phosphatized sediments, otolith
	FG15–2		Sr	0.002	+	<0.1					2				Nodule fragments
418	G182	Siliceous clay	Sr	0.123	⊕	0.3				3	33	90		1.7–1.8	Clay, nodule fragments, phosphatized sediments
	FG16–1		Sr	0.138	△	1.1			1	6	19	3		1.73–1.8	〃
	FG16–2		Sr	0.052	⊕	0.4				2	15	2		1.79	〃
419	G183	Deep sea clay	SPr	1.620	△	3.2			1	118	86	>200		1.87–1.90	Phosphatized sediments, nodule fragments
	FG17–1		SPr	0.820	◬	6.3			1	50	101			1.85–1.98	〃
	FG17–2		SPr	0.765	◬	5.9				59	97			1.94–1.96	〃
420	G184	Siliceous clay	Sr	0.008	+	<0.1					3	14		1.78	
421	G185–1	Calcareous ooze	Crust												
422	G186	Siliceous clay	Sr	0.015	+	<0.1					7	9		1.8	

423	G187	Siliceous clay	Sr	0.249	⊕	0.5		1	7	82	119	1.79–1.88	Phosphatized sediments
	FG19–1		Sr	0.066	⊕	0.5			3	22	20	1.85–1.90	Oxides
	FG19–2		Sr	0.152	△	1.2		1	5	37	20	1.7–1.9	Oxides, clay
424	G188	Siliceous clay	Sr	0.004	+	<0.1				2	1		Clay, oxides fragment
	FG20–2		Sr	0.061	⊕	0.5			6	3	1	1.8–2.0	〃
425	G189	Siliceous clay	Sr		+	<0.1					1		
	FG21–1		Sr	0.002	+	<0.1				1			
	FG21–2		Sr	0.006	+	<0.1			1				
426	G190	Deep sea clay	Sr	0.706	△	1.4		2	35	20	30	1.93–2.04	Clay, oxides particles
	FG22–1		Sr	0.621	△	4.8		2	27	10	22	1.97–2.06	〃
	FG22–2		Sr	0.177	△	1.4			11	10	12	1.83–1.94	〃
427	G191	Siliceous clay	Sr		+	<0.1					1		
	FG23–1		Sr		+	<0.1					1		
429	P72	Deep sea clay	Ss/SPs	0.002						1			
	FG27–1		Ss/SPs, ISs	1.269	◬	9.1	1	22	10	1	1	1.94–2.0	Composit phosphatized and cherty sediments
	FG27–2		Ss/SPs	1.085	◬	8.3		17	21			1.92–2.0	〃
430	G195	Deep sea clay	Ss/SPs, V(f.)	5.089	◉	10.2	1	46	223	103	75	1.96–2.2	Phosphatized sediment particles
	FG28–1		Ss/SPs	1.346	◉	10.4	2	9	60	30	25	1.98–2.10	〃
	FG28–2		Ss/SPs	1.706	◉	13.1	1	19	58	46	40	2.00–2.06	〃
431	G196	Siliceous clay	Sr	0.103	⊕	0.2			10	13	3	1.7–1.9	Clay, phosphatized sediment particles
	FG29–1		Sr	0.119	⊕	0.9			6	19	2	2.05–2.1	〃
	FG29–2		Sr, Db	0.311	△	2.4	1		8	16	4	2.0	〃
432	FG30–1	Deep sea clay	Sr	0.038	⊕	0.3			4	2			
	FG30–2		Sr	0.022	⊕	0.2			1	3		2.0	
433	FG31–1		Sr, Db	0.563	△	4.3	1	3	18	8	8	2.0–2.19	Phosphatized sediment particles, fossils
	FG31–2		Sr, Db	0.217	△	1.7	1		3	5		2.03–2.2	〃

+ <0.1, ⊕ 0.1–1.0, △ 1.0–5.0, ◬ 5.0–10.0, ◉ 10.0–20.0, ● >20 kg/m²

Table XIV-2 Morphological classification of manganese nodules.

Types	Size	Shape	Surface texture	MEYER (1973)	MAYLAN (1974)
Sr	small-medium	spheroidal/ellipsoidal	rough (granular or microbotryoidal)	Kr	s-m[S, E]r
SPr	small-medium	spheroidal/ellipsoidal/ intergrown	rough	Kr	s-m[S, E, P]r
SEr	medium-large	spheroidal/ellipsoidal	rough-botryoidal	B	m-l[S, E]r
Db	medium-large	discoidal/ellipsoidal	rough-botryoidal	B	m-l[D, D-E]r
Ss/SPs	small-medium	spheroidal/intergrown	smooth (smooth or microgranular)	Kg	s-m[P, S, E]s
DPs	small-medium	flattened/elongated/ discoidal/intergrown	smooth	Kg	s-m[D, P, E]s
ISs	large	irregular/spheroidal/ flattened/angular/ fractured	smooth	G	l[S, F]s
IDPs	large	irregular/flattened/ discoidal/fractured	smooth		l[D, T, P, F]s
V	small-large	variable depending on the nucleus forms (Shark's teeth, nodule fragments etc.)	smooth or rough	KRU	s-m-l[B, F]r, s

Each type name is represented by the symbols taken from the initial of each morphological term, mostly applying the Meylan/Craig's classification method (Meylan, 1974). Here, each size class roughly corresponds in maximum diameter; small- <4 cm, medium- 4-6 cm, large- >6 cm. Morphological symbols indicate; S- spheroidal, E- ellipsoidal, D- discoidal, P- poly or intergrown, I- irregular, V- variable, F- faceted, B- biological, T- tabular or flattened.

texture on the buried parts and smooth ones on the exposed parts. Also, some nodules have a more rough and knobby pronounced structure along their equatorial rims, which are just in contact with the interface.

It is likely that this rough texture reflects the growing state of the nodule. The smooth surface indicates a rather slow growth or erosion of the nodule, and the knobby equatorial part results from more active horizontal growth.

As above stated, though each individual nodule has more or less both a rough surface at the bottom and a smooth surface at the top, it still has a predominantly rough or smooth appearance as a whole. According to this total feature, nodules are grouped into two basic types, smooth (s) types and rough (r) types including botryoidal ones. From the nodule occurrence at sediment-water interface, the r type is buried relative to the s type which are more exposed.

Shape

The most common shapes of nodules are either ideal individual forms of spheroidal, ellipsoidal, discoidal, etc. or polylobate or intergrown aggregate forms (Sr, SPr, SEr, Db, Ss/SPs, DPs).

An interesting example is the mode of occurrence of the ISs and IDPs types. These

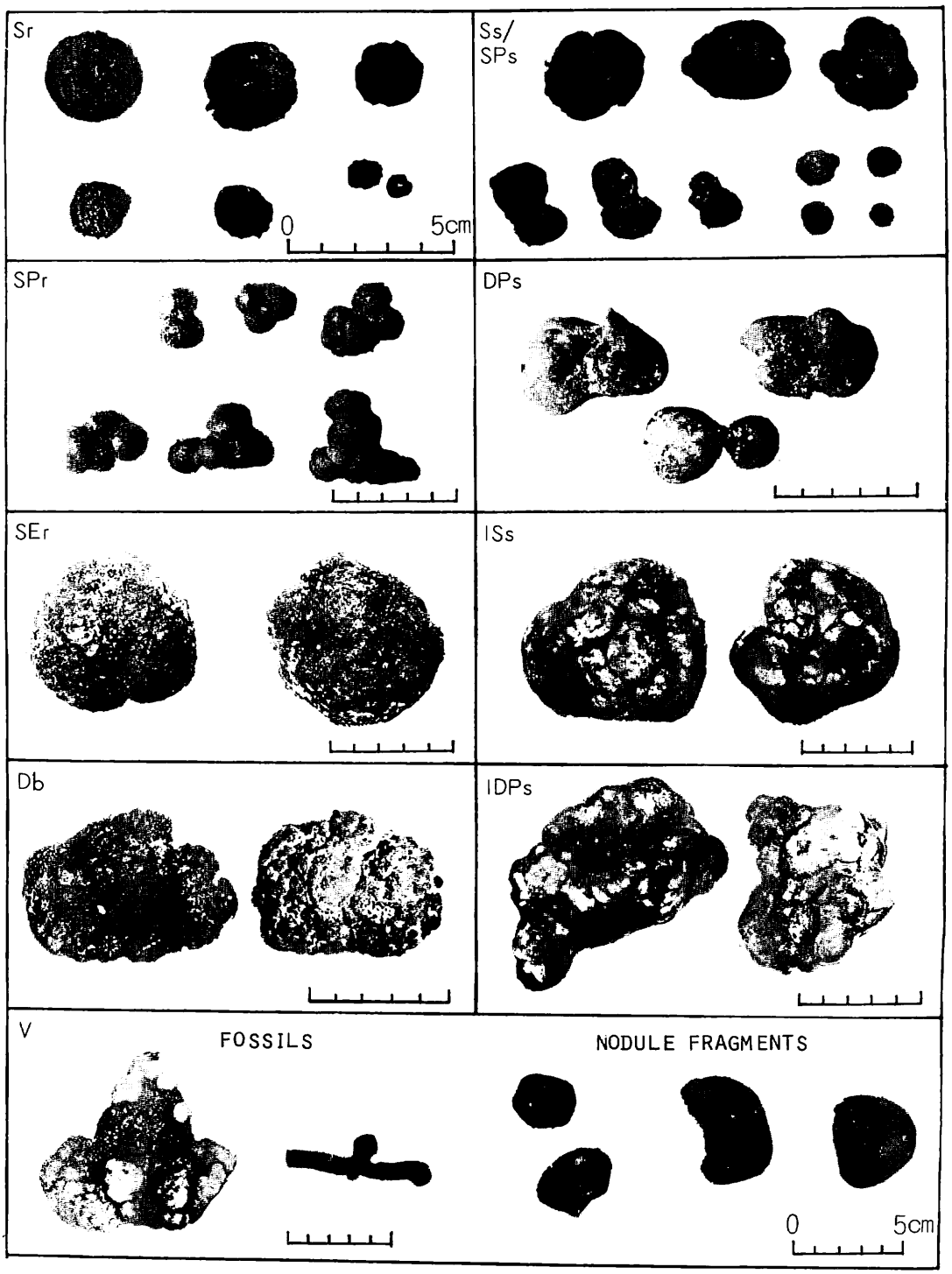

Fig. XIV-1 Morphological types of manganese nodules.

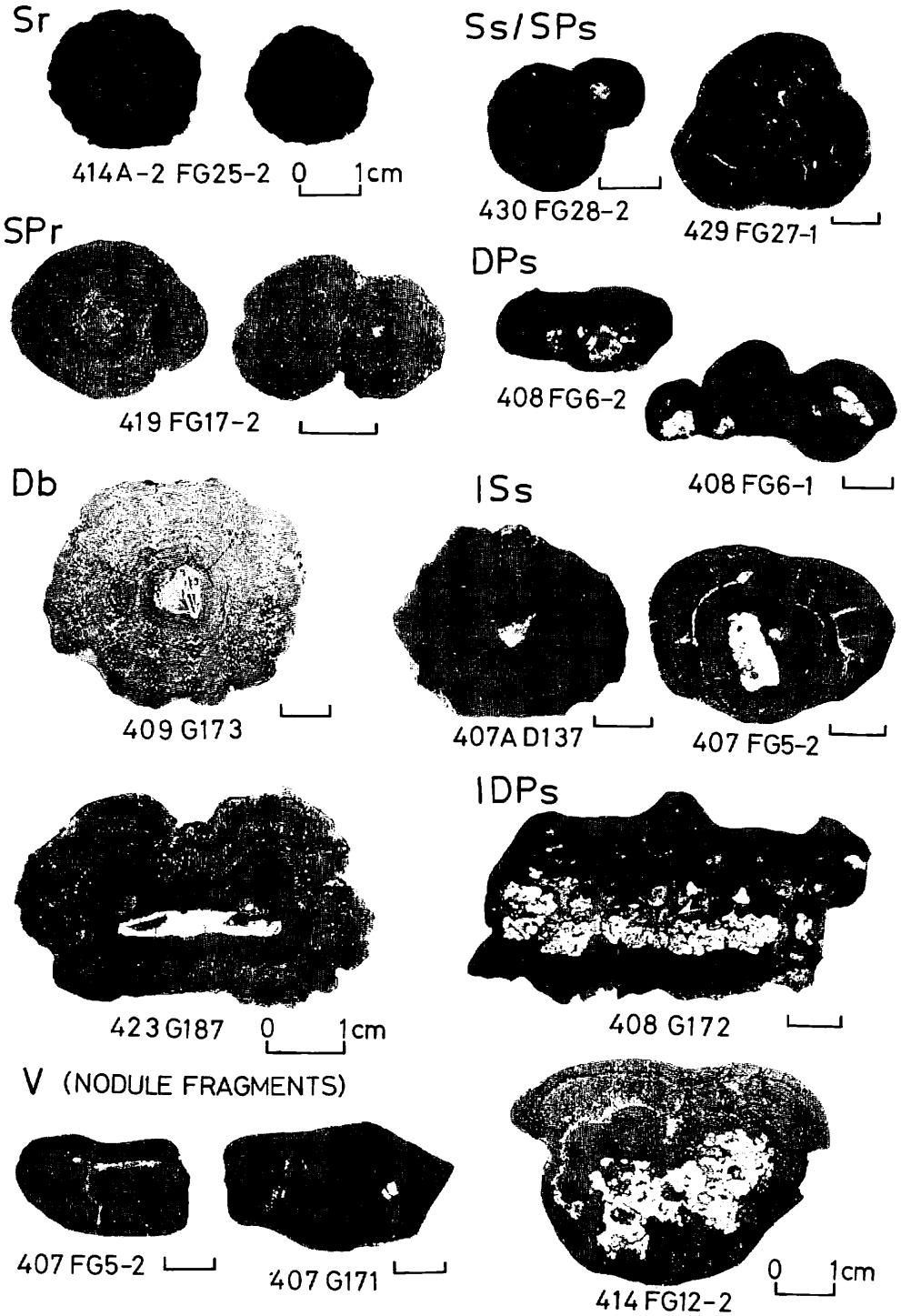

Fig. XIV-2 Internal structure of manganese nodules of each type.

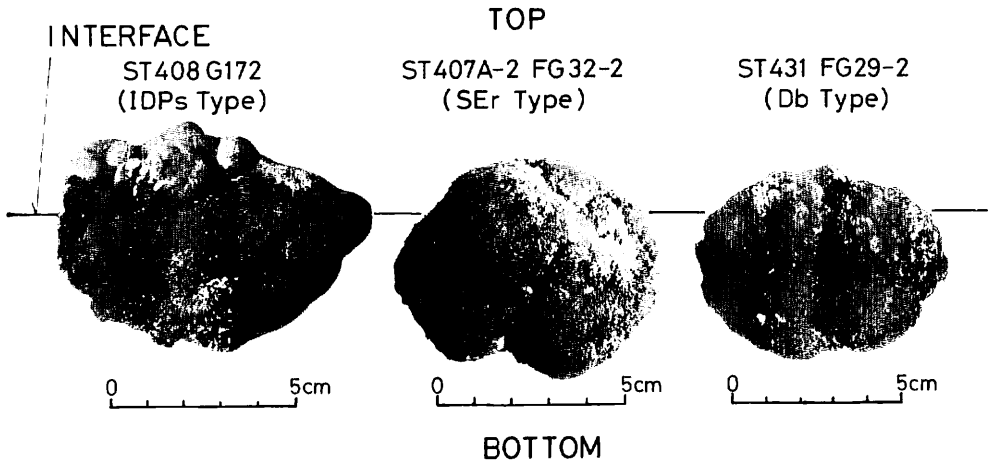

Fig. XIV-3 Occurrence and surface texture of nodules in relation to sediments-water interface.

types seem to indicate that they were originally in a complete or ideal form of spheroidal (S), ellipsoidal (SE) or discoidal (D)/polylobate or intergrowth (P) shapes, but now are in an incomplete form due to breakup of several or larger parts of nodules so that the fractured surface is coated by a thin younger oxide layer.

These type nodules are usually accompanied with V type nodules with fractured fragment cores of older nodules.

The irregular broken type nodules tend to occur in densely populated areas as evidenced in some of the sea-floor photographs. This suggests relationship between the breakup of the nodules and their overpopulation, though probable causes such as the shrinkage and generation of fracturing as an internal factor and bottom current effect as an external factor (RAAB, 1972) may be important.

Besides the nodule fragments, the variable form V type includes rock fragments, shark's teeth and other animal bones as their nuclei.

Internal structures

Internal structures of the nodules appear to differ according to nodule types (Fig. XIV-2). Generally, r type nodules lack a nucleus or have small ones, and dendritic colloform structures are developed along the outer surface zone of the nodule, resulting in a rough surface texture. Sr, SPr, and SEr types have concentrically layered bands, and the Db type has asymmetric concentric bands elongated towards the edges.

The s type nodules, such as Ss/SPs, DPs, especially the ISs and IDPs types often contain fractures, which are radial or parallel to concentric bands and usually thin out towards the outer surface zone. Among these types, the Ss/SPs type has concentric bands and small nuclei similar to that of the r type nodules. Many of the ISs and IDPs types consist of internal massive or less clear banded blocks of older nodules and an outer younger thin (2–3 mm thick) oxide layer coating. Also, the nuclei of these types, in many cases consist of an intergrown aggregation of small pisolitic nodules or larger size sedimentary fragments. The materials of fragmental nuclei of the nodules are volcanic rock, pumice, mud sediments (often phosphatized), fossils, and older nodules.

Size

Although each type has a wide range of size, there are some tendencies recognized in the size distribution. Sr, SPr, Ss/SPs, and DPs types of spheroidal, ellipsoidal, and intergrown form are of small-medium size. SEr and Db types are medium-large size as the larger types of the former, but their occurrence is restricted in number. The irregular types of ISs and IDPs are, however, large of size, and in areas with a high nodule population.

Relationship between nodule types and chemical and mineralogical composition

As described in Chapter XVI, notable relationships are recognized between nodule types and chemical composition. According to the fundamental two types based on surface texture, rough (r) and smooth (s) types, the contents of the main components differ. The r types are rich in Mn, Cu and Ni, while the s types are rich in Fe and Co. Besides, there is a conversely changing tendency of those groups, a decreasing Mn, Cu, and Ni group and an increasing Fe. Co group related to a series of types in the order of Sr→SPr→Ss/SPs→DPs→ISs→IDPs. This coincides with the established tendency described by MEYER (1973), but the Db type, presumably corresponding to his "B" type, with the highest Mn, Cu and Ni contents does not necessarily show a higher value in our one analysis. More data is needed about this.

According to M. NOHARA (see Chap. XV of this report,), 10 Å manganite (todorokite) and δ-MnO_2 (Birnessite) are identified by X-ray diffractometer and a brown material rich in iron oxide and clay mineral is distinguished by microscopic observation in nodules.

Of the two manganese minerals, 10 Å manganite is more commonly found. However, the relationship between nodule type and mineral composition is not clear yet because of the lack of quantitative data on the complete mineralogy of individual nodules. Nevertheless, it is very suggestive that 10 Å manganite is formed in close connection with interstitial water rich in minor elements such as Ni, Cu, etc., while δ-MnO_2 is formed by precipitation from sea water (USUI, 1976). According to this mechanism, it is likely that the buried r type nodules are enriched in Mn, Cu and Ni, and this depends on the abundance of 10 Å manganite in the mineral composition.

Thus, there is the possibility that the relationship between nodule types, chemistry, and mineralogy is explained in terms of the conditions of nodule formation, i.g., sedimentary environment and supply of metal elements. This problem is worthy of further investigation.

Distribution of nodules

A map of the regional distribution of nodule types and their abundance in the surface sediment is shown in Fig. XIV-4. As described in Chapter X, the deep sea clay, presumably of Tertiary age, occupies a wedge-shaped area extending from northwest to southeast. This deep sea clay is overlain mostly by some 20 cm of siliceous clay of Quaternary age and partly by siliceous/calcareous clay of the same age but of different facies.

The relationship between nodule type, their abundance, and sediment types may be summarized as follows. Rough surface types are distributed widely throughout the areas of both siliceous and deep sea clay, but their abundance is generally small. Smooth

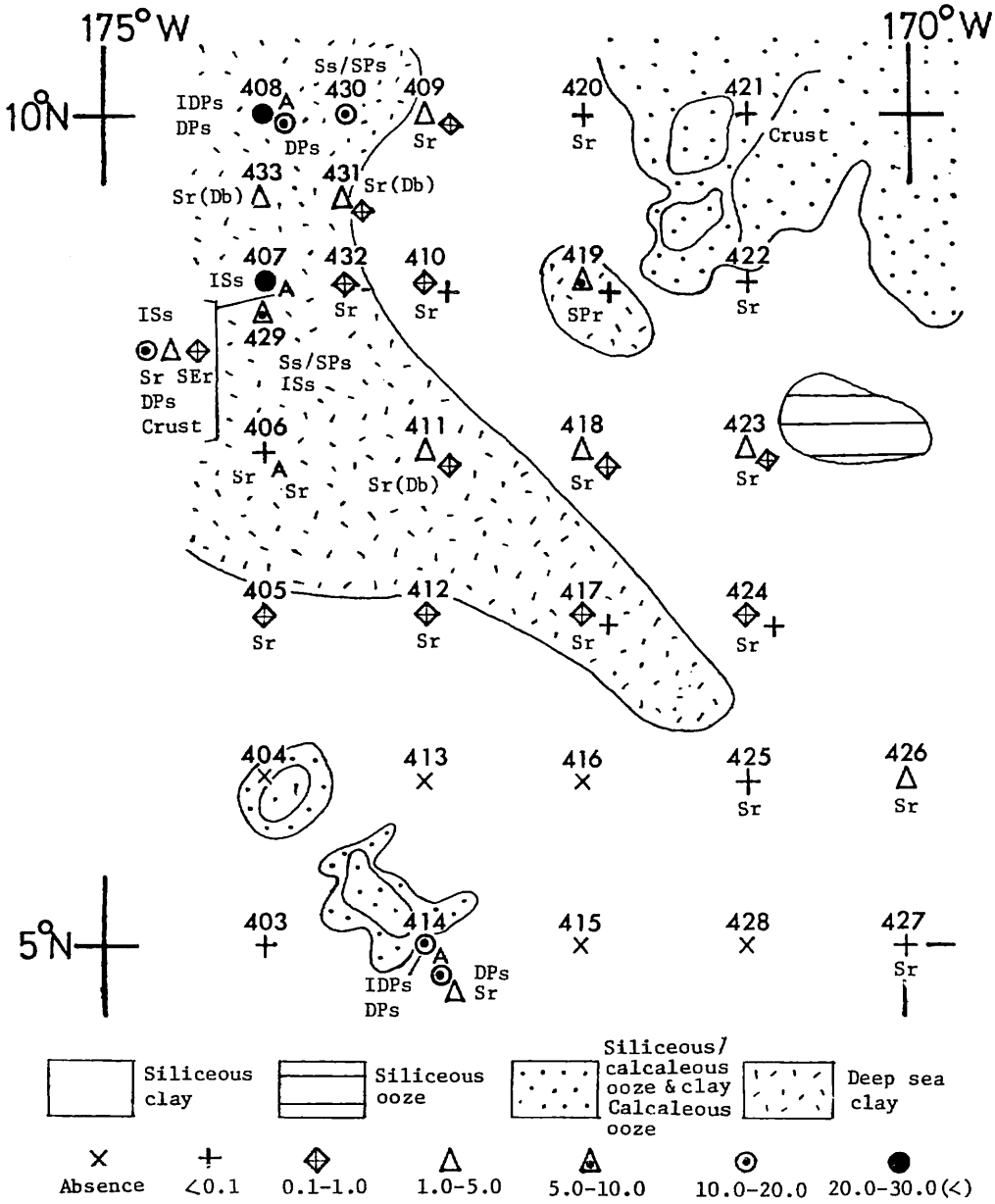

Fig. XIV-4 Distribution of surface sediments, manganese nodules and their abundance (population density). Population density is shown in kg/m², and two different marks of it in one station indicate variation of its values accoding to the different sampling points within the same station area.

surface types are confined to the areas of deep sea clay and the boundary zone between siliceous clay and siliceous/calcareous clay. Their abundance is larger and the highest population density of the order of 30 kg/m^2 is found in the northwestern part of the deep sea clay area.

The Sr type nodules are widely distributed and occur at almost all the stations. Next, in degree of areal distribution, are the SEr and Db types, which occur as larger size nodule associated with smaller numbers of the Sr type. The Db type was found in the Sts. 441, 423, 426, 431, and 433. SPr type nodules also occur together with the Sr type, and were abundant at St. 419. The s type group nodules have a rather restricted distribution in the northwestern basin and the southwestern "St. 414 Deep Sea Hill" areas. They were collected from the following stations respectively: Ss/SPs type at Sts. 429 and 430; DPs type at Sts. 407, 407A, 408, 414A; ISs type at Sts. 407 and 407A and a similar type partly at St. 429 and 430; and IDPs type at Sts. 408 and 414.

The V type nodules, with nodule fragment cores, were found at Sts. 407 and 407A in particular. Other V types with nuclei of animal fossils such as Shark's teeth were disseminated in hauls from several stations.

The above-stated tendencies of nodule distribution are concerned with stations separated by a distance of about 100 km or 50 km. In order to check the continuity of nodule types, the chemical composition and abundance of nodules within a limited area, detailed examination on the distribution of nodule types at each of the stations on the basis of systematic and close distance sampling was tried at St. 407 or St. 414. The results show that the s type nodules are the major type at these stations and vary abruptly into clear Sr type nodules even over small distances. This suggests a probable relationship between nodule type and environmental factors such as topography and bottom conditions.

In conclusion, the nodule types are likely to reflect the geological environment and conditions of nodule growth, such as topography, sediment type, bottom current, supply of metal elements, interstitial water, and other geochemical factors. For this reason, it is necessary to study further the types and their relation to the geological conditions, on the basis of both wider and more detailed sampling.

References

MEYLAN, M. A. (1974) Field description and classification of manganese nodules. *In* ANDREWS, J. E., *et al.*, "Ferromanganese deposits of the ocean floor", Cruise Report MN-74-01, R/V MOANA WAVE, Honolulu to San Diego, 17 July to 10 August, 1974, *Hawaii Institute of Geophysics Report* HIG-74-9, Honolulu, p. 158–168.

MEYER, K. (1973) Surface sediment and manganese nodule facies, encountered on R/V "Valdivia" cruises 1972/1973. *Meerestechnik*, vol. 4, p. 196–199.

RAAB, W. (1972) Physical and chemical features of Pacific deep sea manganese nodules and their implications to the genesis of nodules. *In* HORN, D. R. (*ed.*), *"Papers from a conference on ferromanganese deposits on the ocean floor,"* Arden House, Harriman, New York and Lamont-Doherty Geological Observatory, Columbia University, 1972, p. 31–49.

USUI, A. (1976) Constituent minerals of manganese nodules. *Marine Science/ Monthly* (Tokyo), vol. 8, p. 751–756 (in Japanese).

Fig. XIV-5 (1–24) Photograph log of manganese nodules of each station.
(1)Scale of unit areas and grid plane, on which nodules were photographed.
Larger frame ($0.7m \times 0.7m = 0.5m^2$) represents an area caught by Ocean−70 grab sampler, and smaller frame ($0.34m \times 0.34m = 0.13m^2$) shows that by Freefall grab sampler. Photographs on the right side are of selected samples representing size and morphology. Scale of grid span is 5cm.

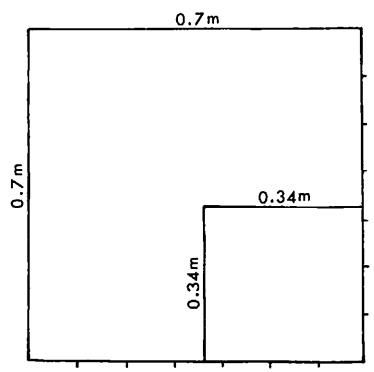

(1)

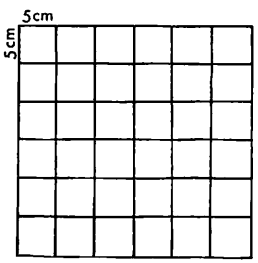

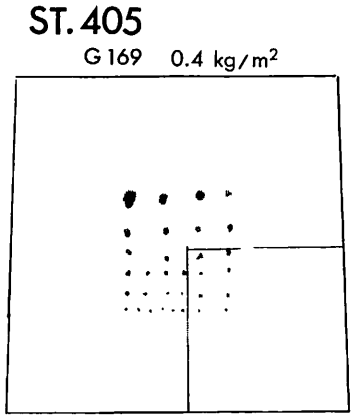

(2)

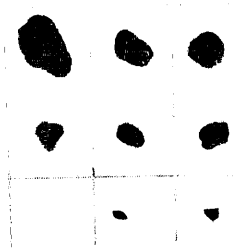

ST. 407

G 171 30.0 kg/m²

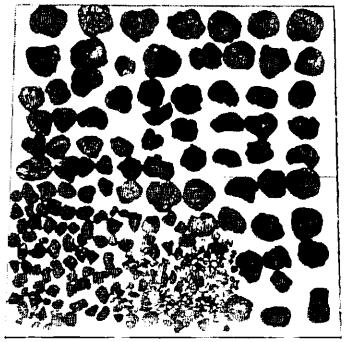

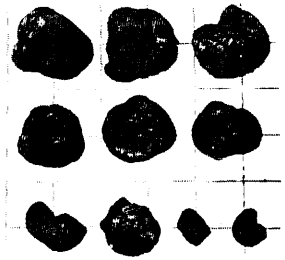

FG 5-1 29.2 kg/m²

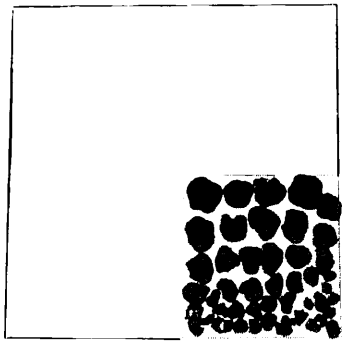

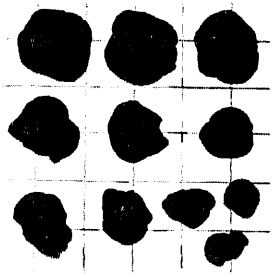

FG 5-2 29.2 kg/m²

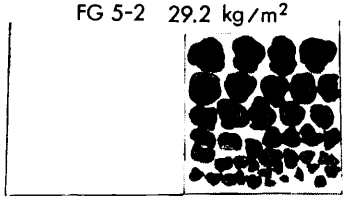

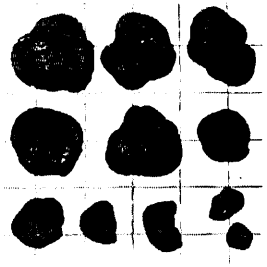

(3)

ST. 407A

D 137

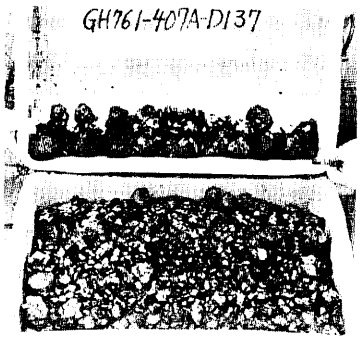

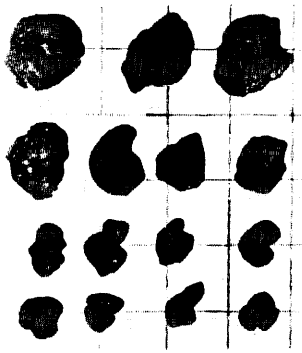

(4)

ST. 407A-2

FG 32-1 0.8 kg/m²

FG 32-2 17.5 kg/m²

FG 32-3 1.2 kg/m²

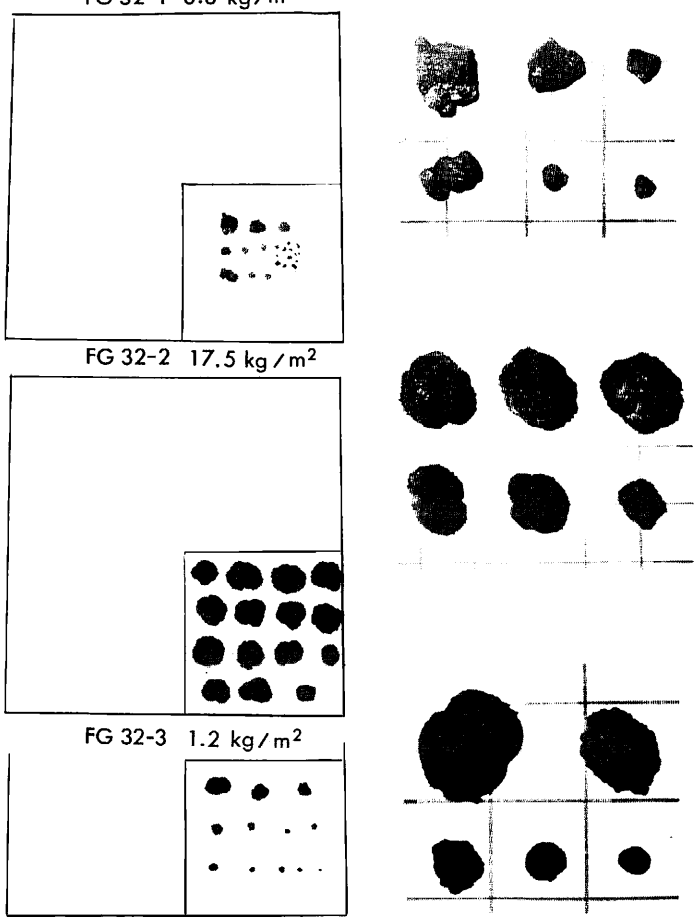

(5)

ST. 407A-2

FG 32-4 0.3 kg/m²

FG 32-5 0.5 kg/m²

FG 32-6 0.3 kg/m²

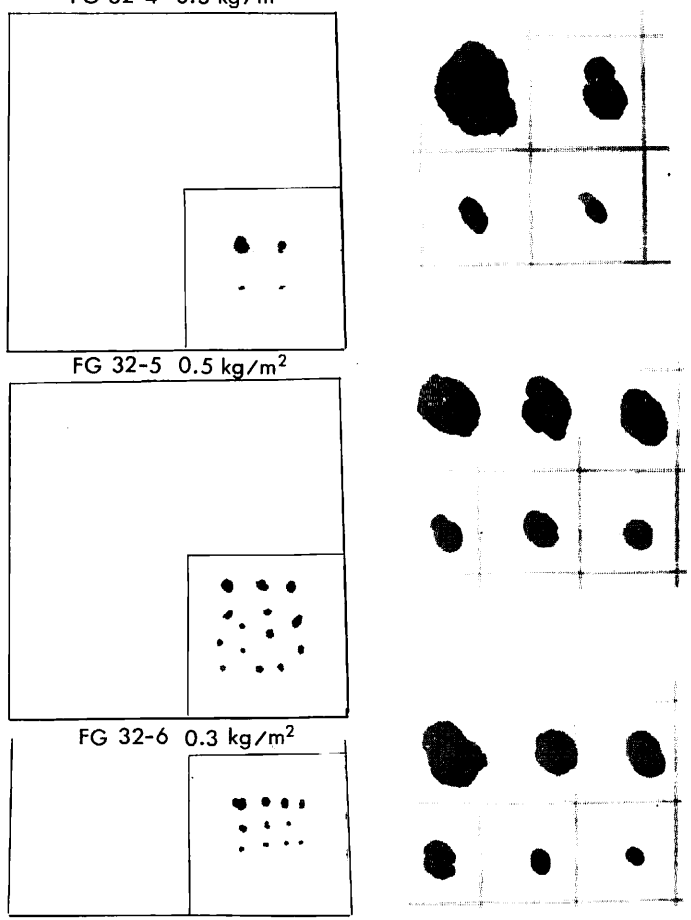

(6)

ST. 407A-2

FG 32-7 1.3 kg/m^2

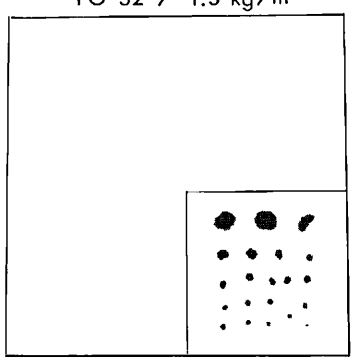

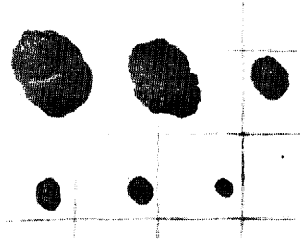

FG 32-8 1.3 kg/m^2

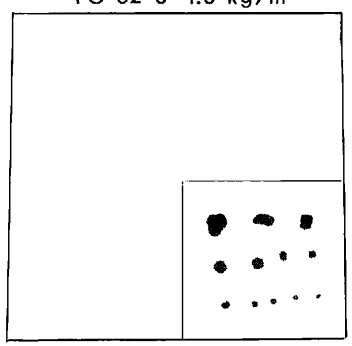

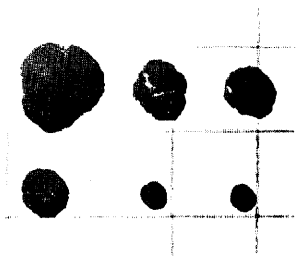

(7)

ST. 408

G 172 11.8 kg/m^2

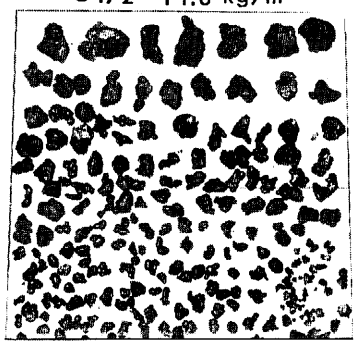

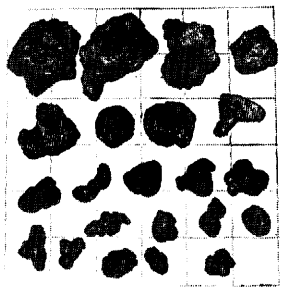

FG 6-1 23.0 kg/m^2

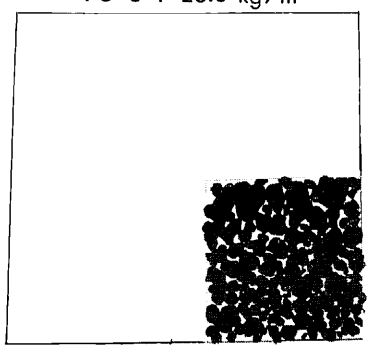

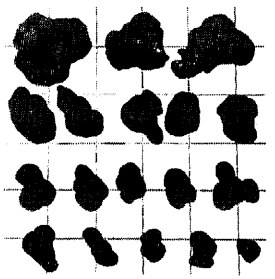

FG 6-2 20.0 kg/m^2

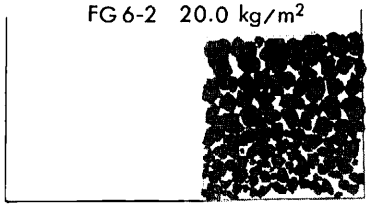

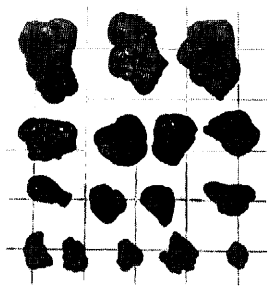

(8)

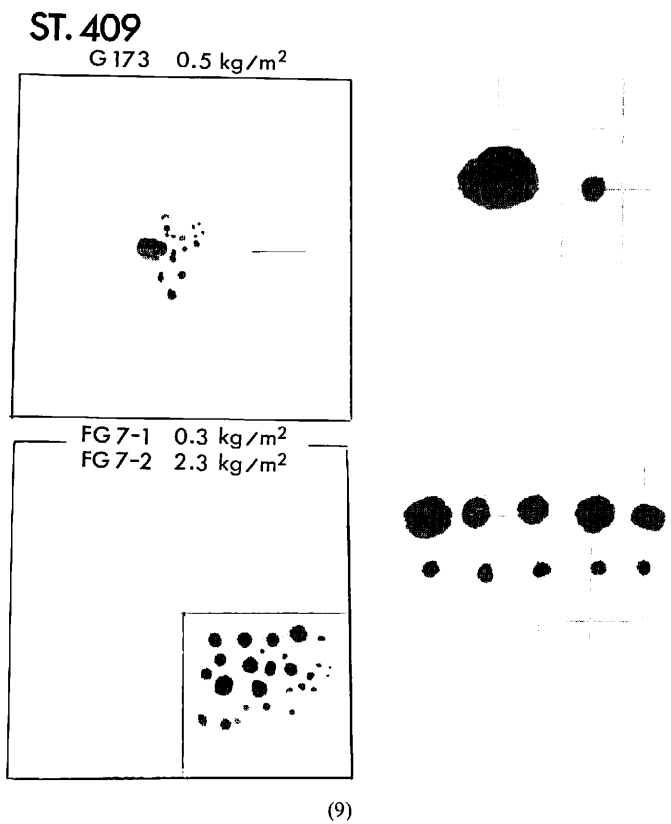
ST. 409
G 173 0.5 kg/m²
FG 7-1 0.3 kg/m²
FG 7-2 2.3 kg/m²

(9)

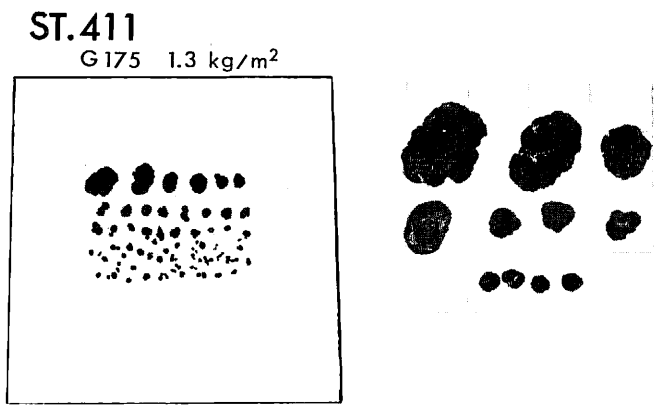
ST. 411
G 175 1.3 kg/m²

(10)

ST. 414

FG 12-1 16.4 kg/m²

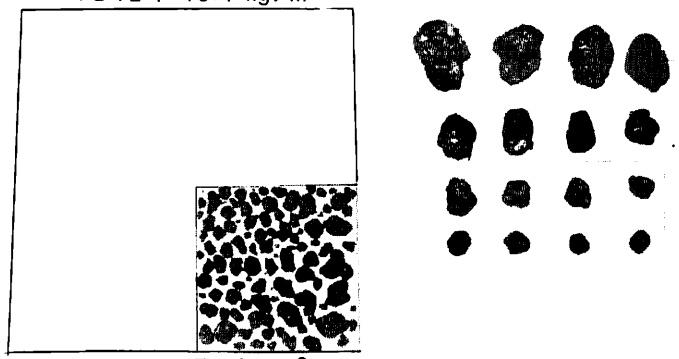

FG 12-2 17.2 kg/m²

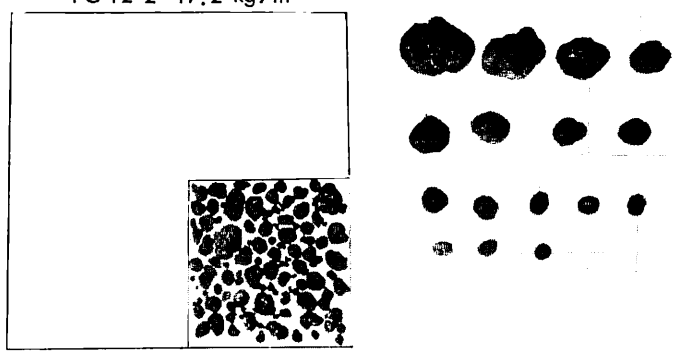

(11)

ST. 414-A

G 193 10.7 kg/m²

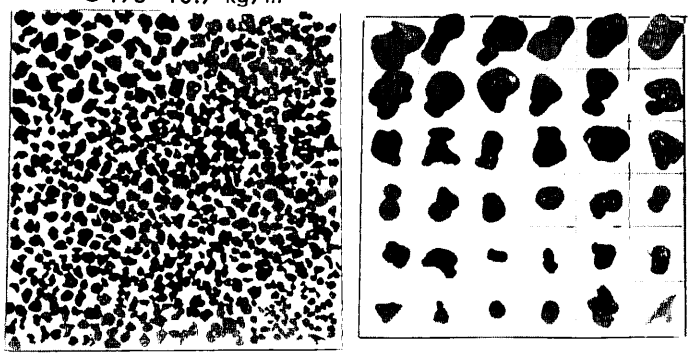

ST. 414-A-2

FG 25-1 2.2 kg/m²

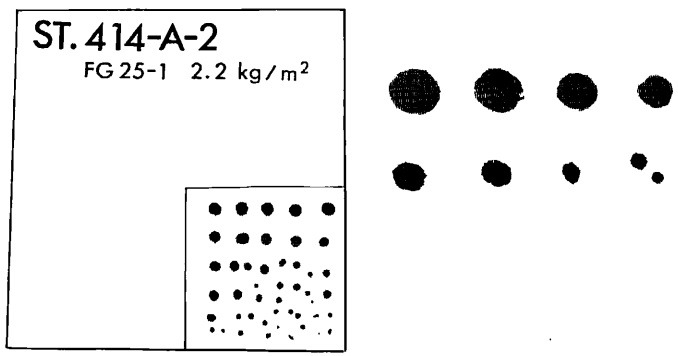

FG 25-2 3.5 kg/m²

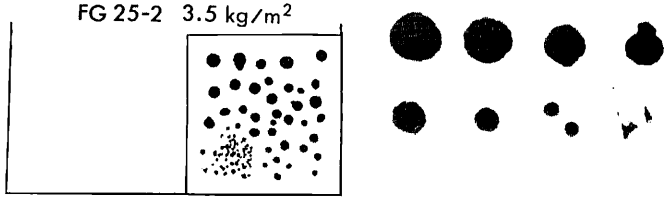

(12)

ST. 417

G 181 0.3 kg/m²

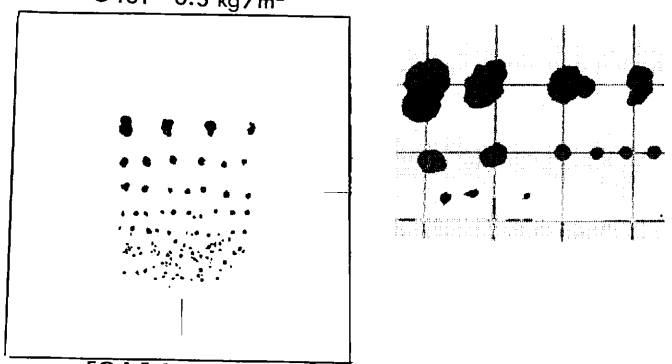

FG 15-1 0.8 kg/m²

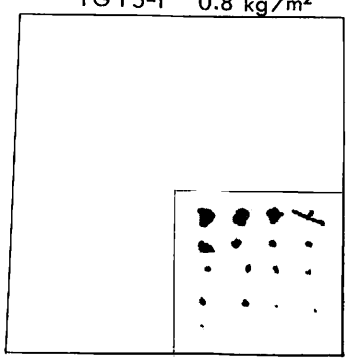

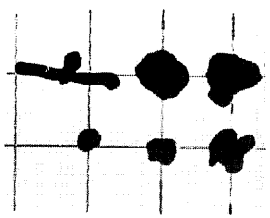

FG 15-2 <0.1 kg/m²

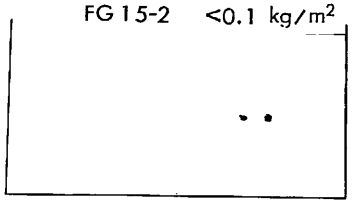

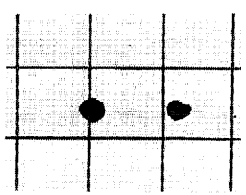

(13)

ST. 418

G 182 0.3 kg/m²

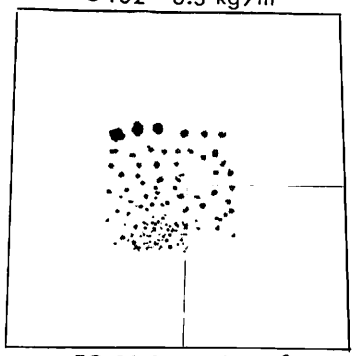

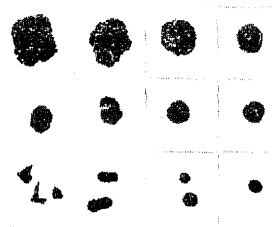

FG 16-1 1.1 kg/m²

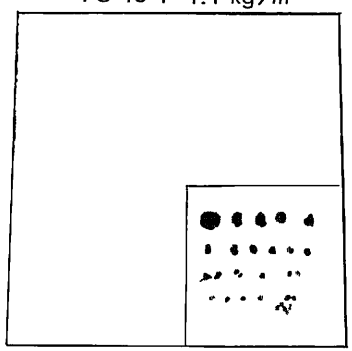

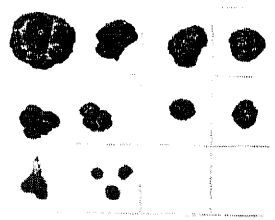

FG 16-2 0.4 kg/m²

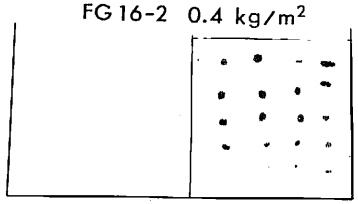

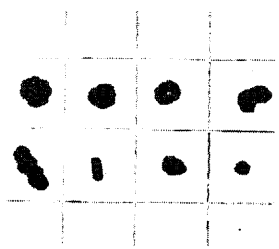

(14)

ST. 419

G183 3.2 kg/m²

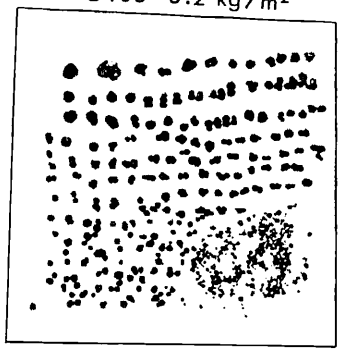

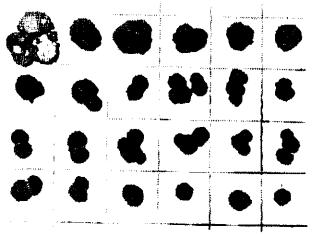

FG 17-1 6.3 kg/m²

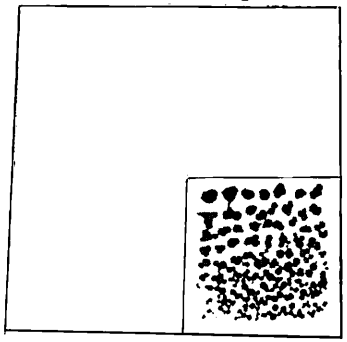

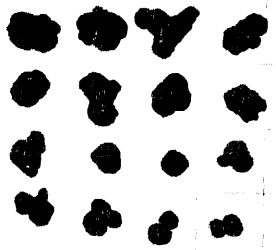

FG 17-2 5.9 kg/m²

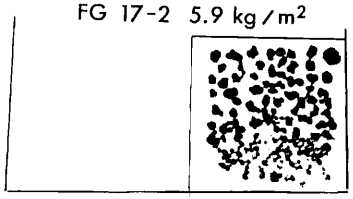

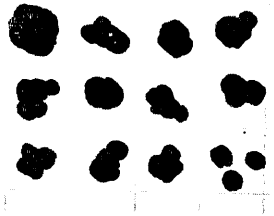

(15)

ST. 420

G184 <0.1 kg/m²

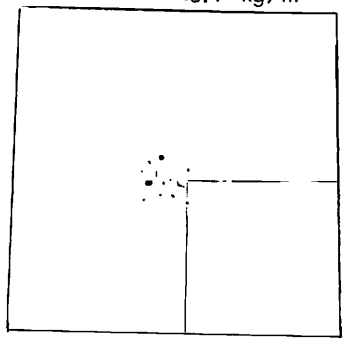

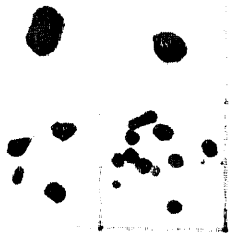

ST. 422

G186 <0.1 kg/m²

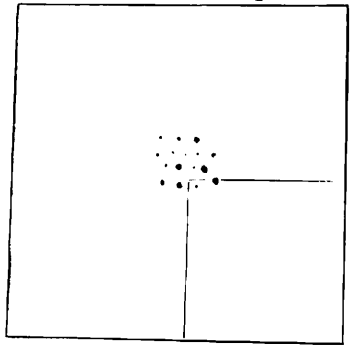

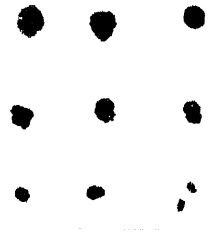

(16)

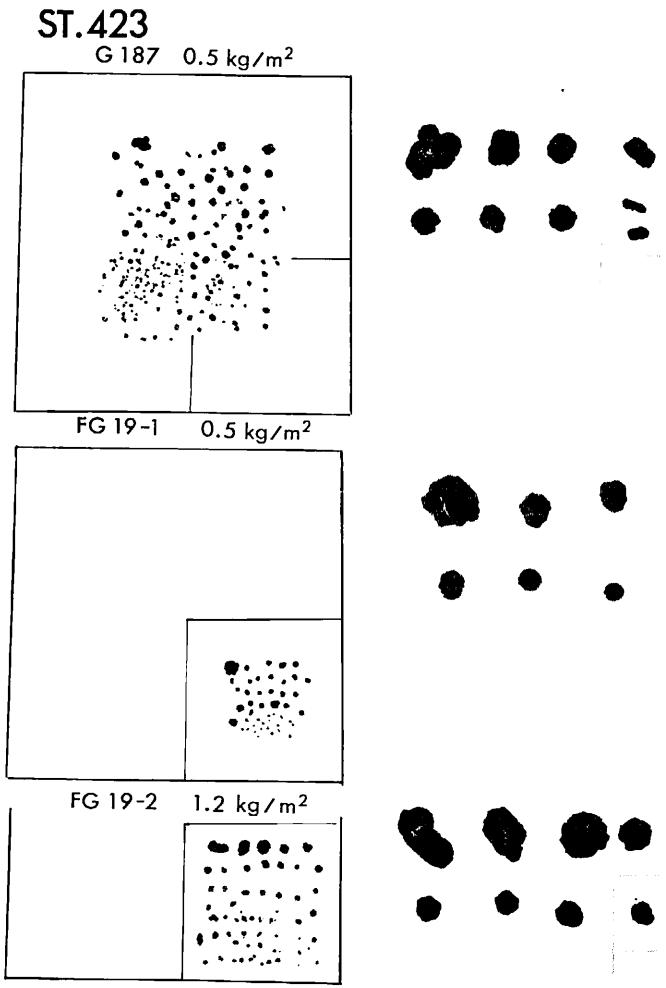
ST. 423
G 187 0.5 kg/m²
FG 19-1 0.5 kg/m²
FG 19-2 1.2 kg/m²

(17)

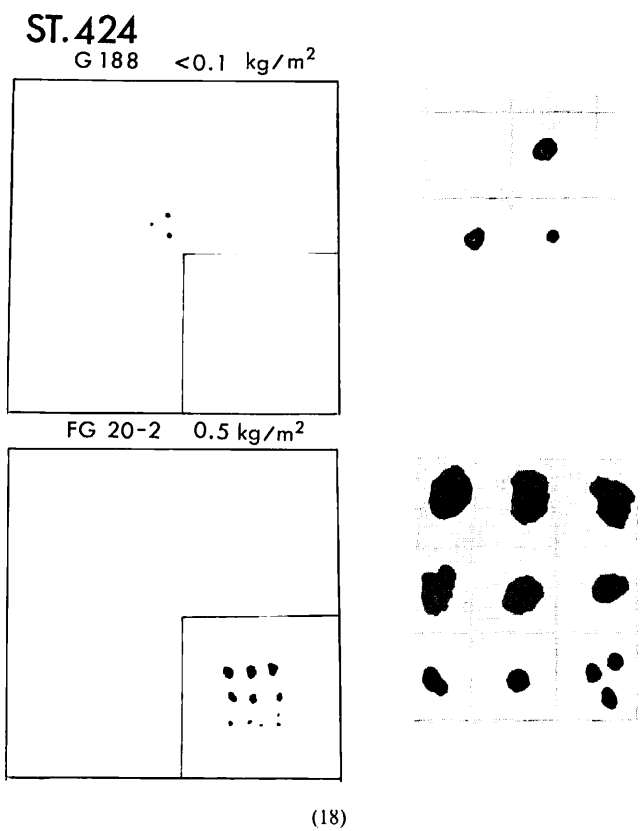
ST. 424
G 188 <0.1 kg/m²
FG 20-2 0.5 kg/m²

(18)

ST. 426

G 190 1.4 kg/m^2

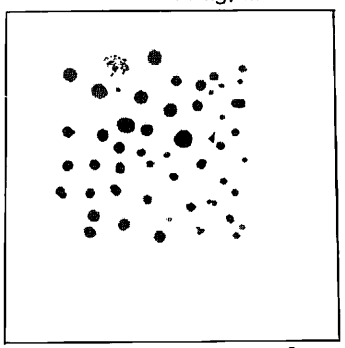

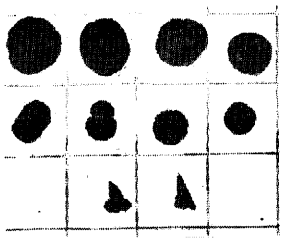

FG 21-1 4.8 kg/m^2

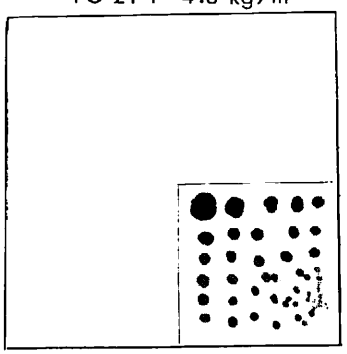

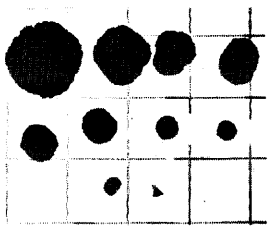

FG 21-2 1.4 kg/m^2

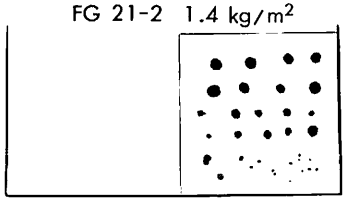

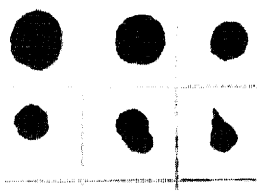

(19)

ST. 429

FG 27-1 9.1 kg/m^2

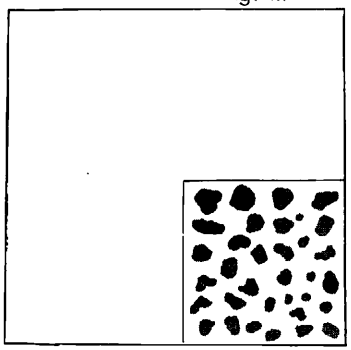

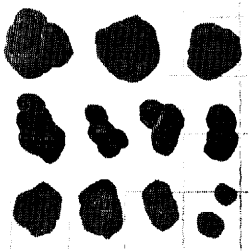

FG 27-2 8.3 kg/m^2

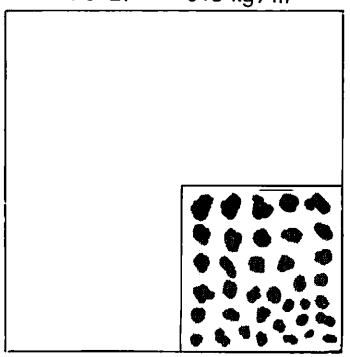

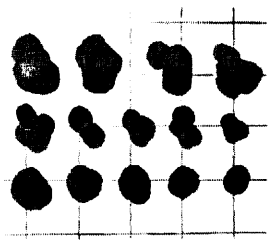

(20)

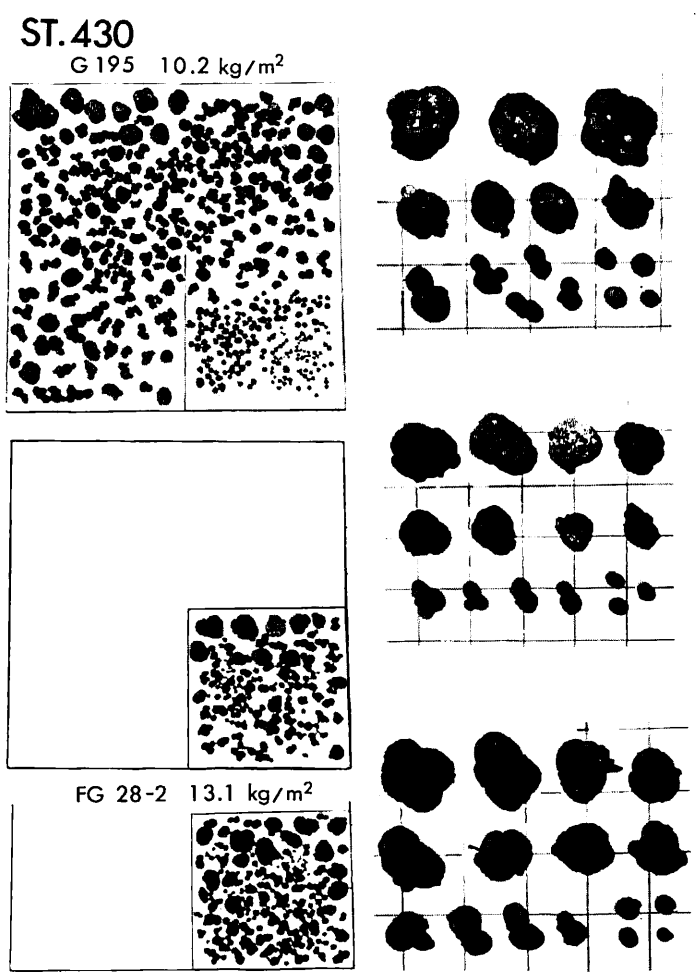
ST. 430
G 195 10.2 kg/m²
FG 28-2 13.1 kg/m²

(21)

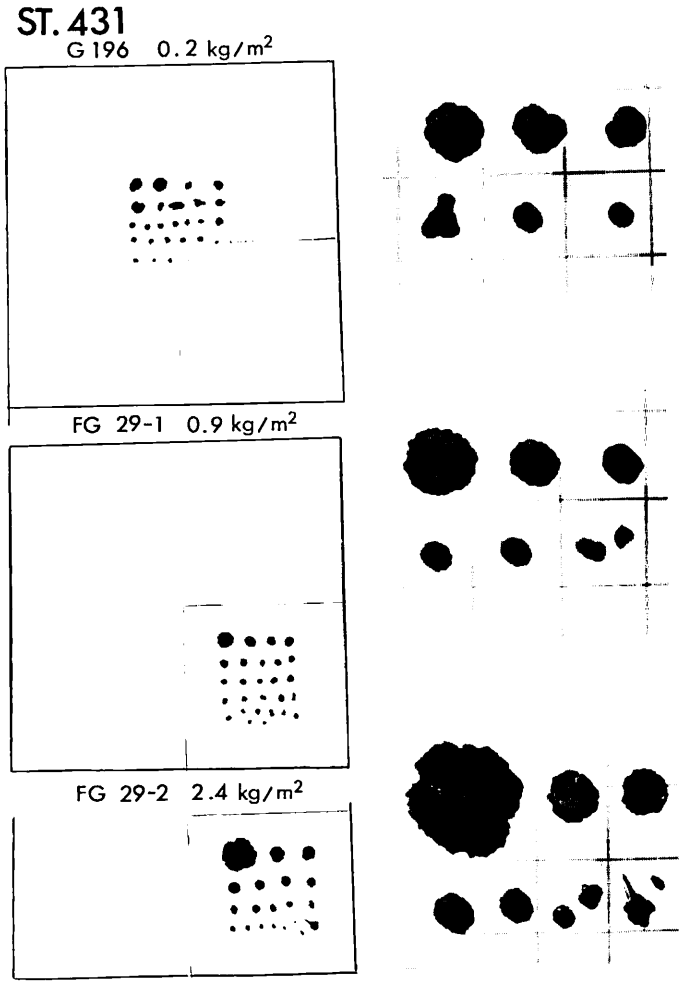
ST. 431
G 196 0.2 kg/m²
FG 29-1 0.9 kg/m²
FG 29-2 2.4 kg/m²

(22)

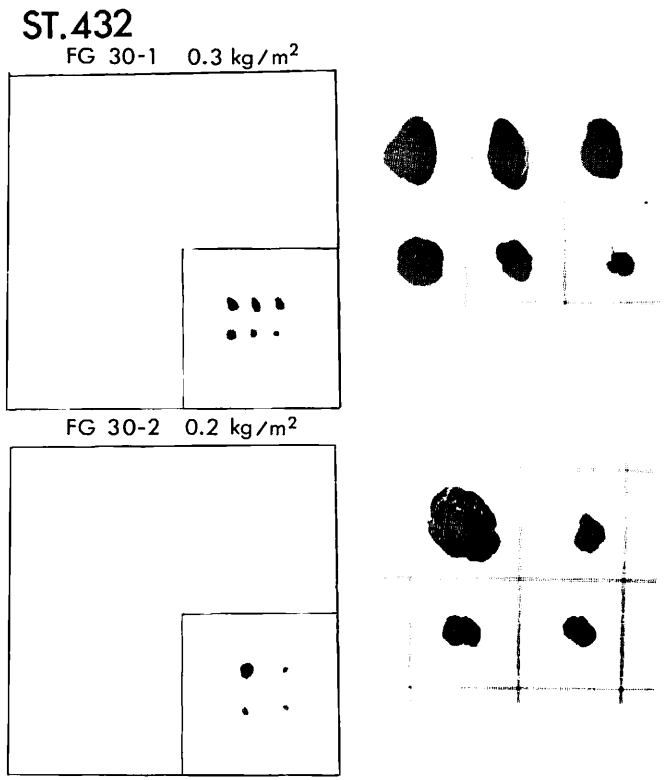
ST. 432
FG 30-1 0.3 kg/m²
FG 30-2 0.2 kg/m²

(23)

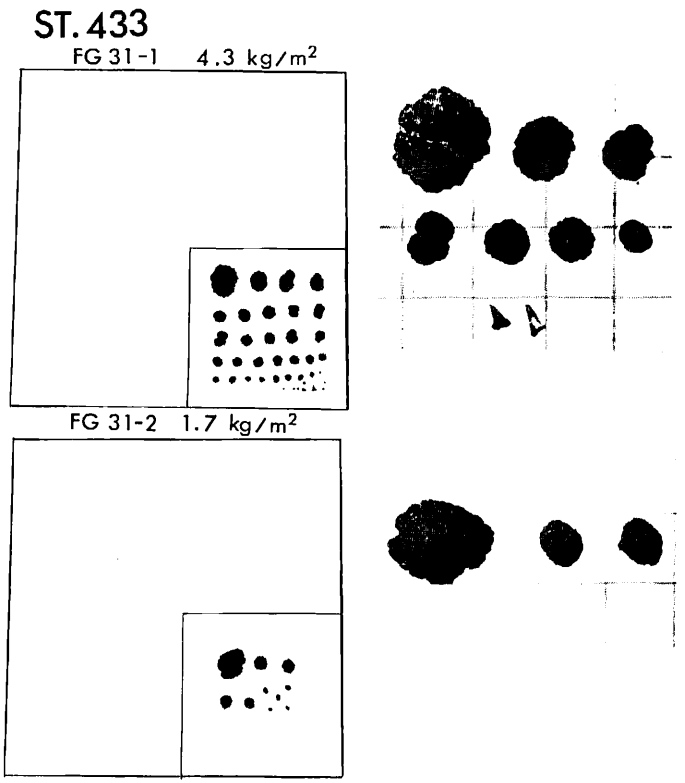
ST. 433
FG 31-1 4.3 kg/m²
FG 31-2 1.7 kg/m²

(24)